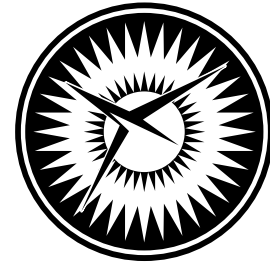


NASA/CR-2007-213926  
NIA Report No. 2005-08



NATIONAL  
INSTITUTE OF  
AEROSPACE



# Quasi-Linear Parameter Varying Representation of General Aircraft Dynamics Over Non-Trim Region

*Jong-Yeob Shin*  
*National Institute of Aerospace, Hampton, Virginia*

---

February 2007

## The NASA STI Program Office . . . in Profile

Since its founding, NASA has been dedicated to the advancement of aeronautics and space science. The NASA Scientific and Technical Information (STI) Program Office plays a key part in helping NASA maintain this important role.

The NASA STI Program Office is operated by Langley Research Center, the lead center for NASA's scientific and technical information. The NASA STI Program Office provides access to the NASA STI Database, the largest collection of aeronautical and space science STI in the world. The Program Office is also NASA's institutional mechanism for disseminating the results of its research and development activities. These results are published by NASA in the NASA STI Report Series, which includes the following report types:

- **TECHNICAL PUBLICATION.** Reports of completed research or a major significant phase of research that present the results of NASA programs and include extensive data or theoretical analysis. Includes compilations of significant scientific and technical data and information deemed to be of continuing reference value. NASA counterpart of peer-reviewed formal professional papers, but having less stringent limitations on manuscript length and extent of graphic presentations.
- **TECHNICAL MEMORANDUM.** Scientific and technical findings that are preliminary or of specialized interest, e.g., quick release reports, working papers, and bibliographies that contain minimal annotation. Does not contain extensive analysis.
- **CONTRACTOR REPORT.** Scientific and technical findings by NASA-sponsored contractors and grantees.

- **CONFERENCE PUBLICATION.** Collected papers from scientific and technical conferences, symposia, seminars, or other meetings sponsored or co-sponsored by NASA.
- **SPECIAL PUBLICATION.** Scientific, technical, or historical information from NASA programs, projects, and missions, often concerned with subjects having substantial public interest.
- **TECHNICAL TRANSLATION.** English-language translations of foreign scientific and technical material pertinent to NASA's mission.

Specialized services that complement the STI Program Office's diverse offerings include creating custom thesauri, building customized databases, organizing and publishing research results ... even providing videos.

For more information about the NASA STI Program Office, see the following:

- Access the NASA STI Program Home Page at <http://www.sti.nasa.gov>
- E-mail your question via the Internet to [help@sti.nasa.gov](mailto:help@sti.nasa.gov)
- Fax your question to the NASA STI Help Desk at (301) 621-0134
- Phone the NASA STI Help Desk at (301) 621-0390
- Write to:  
NASA STI Help Desk  
NASA Center for AeroSpace Information  
7115 Standard Drive  
Hanover, MD 21076-1320

NASA/CR-2007-213926  
NIA Report No. 2005-08



# Quasi-Linear Parameter Varying Representation of General Aircraft Dynamics Over Non-Trim Region

*Jong-Yeob Shin*  
*National Institute of Aerospace, Hampton, Virginia*

National Aeronautics and  
Space Administration

Langley Research Center  
Hampton, Virginia 23681-2199

Prepared for Langley Research Center  
under Cooperative Agreement NCC1-02043

February 2007

Available from:

NASA Center for AeroSpace Information (CASI)  
7115 Standard Drive  
Hanover, MD 21076-1320  
(301) 621-0390

National Technical Information Service (NTIS)  
5285 Port Royal Road  
Springfield, VA 22161-2171  
(703) 605-6000

# QUASI-LINEAR PARAMETER VARYING REPRESENTATION OF GENERAL AIRCRAFT DYNAMICS OVER A NON-TRIM REGION \*

Jong-Yeob Shin <sup>†</sup>

## ABSTRACT

To apply linear parameter varying (LPV) control synthesis and analysis to a nonlinear system, it is required that a nonlinear system be represented in the form of an LPV model. In this paper, a new representation method is developed for the construction of an LPV model from a nonlinear mathematical model without the restriction that an operating point must be in the neighborhood of equilibrium points. An LPV model constructed by the new method preserves local stabilities of the original nonlinear system at “frozen” scheduling parameters and also represents the original nonlinear dynamics over a non-trim region. An LPV model of the motion of FASER (Free-flying Aircraft for Subscale Experimental Research) is constructed by the new method.

## NOMENCLATURE

### physical parameters

- $u, v, w$  : X-, Y-, Z-components of aircraft velocity in body axes
- $p, q, r$  : X-, Y-, Z-components of aircraft angular velocity in body axes
- $\phi, \theta, \psi$  : Position angles
- $\alpha, \beta$  : Angle of attack, side-slip angle
- $m, J, g$  : Total mass, moment of inertia matrix, gravity constant
- $V, T$  : Total speed, thrust force
- $L, M, N$  : X-, Y-, Z-component of moment

### control surfaces

- $\delta_e$  : elevator deflection angle
- $\delta_r$  : rudder deflection angle
- $\delta_{ra}, \delta_{la}$  : right and left side aileron deflection angle
- $\delta_{rf}, \delta_{lf}$  : right and left side flap deflection angle

---

\*This work was supported by the National Aeronautics and Space Administration under NASA Cooperative Agreement NCC1-02043.

<sup>†</sup>National Institute of Aerospace (NIA), Hampton, VA 23666

## aerodynamic coefficients

$C_X, C_Y, C_Z$	:	X-, Y-, and Z-component force aerodynamic coefficients in body axis
$C_l, C_m, C_n$	:	Roll, pitch, and yaw moment aerodynamic coefficients
$C_{X_o}, C_{Z_o}, C_{m_o}$	:	Aerodynamic coefficients for X- and Z-forces and pitch moment
$C_{X_q}, C_{X_{\delta_e}}, C_{X_{\delta_{ra}}}$	:	X-force aerodynamic derivatives due to $q$ , $\delta_e$ , and $\delta_{ra}$
$C_{X_{\delta_{la}}}, C_{X_{\delta_{rf}}}, C_{X_{\delta_{lf}}}$	:	X-force aerodynamic derivatives due to $\delta_{la}$ , $\delta_{rf}$ , and $\delta_{lf}$
$C_{Y_\beta}, C_{Y_p}, C_{Y_r}$	:	Y-force aerodynamic derivatives due to $\beta$ , $p$ , and $r$
$C_{Y_{\delta_r}}, C_{Y_{\delta_{ra}}}, C_{Y_{\delta_{la}}}$	:	Y-force aerodynamic derivatives due to $\delta_r$ , $\delta_{ra}$ , and $\delta_{la}$
$C_{Y_{\delta_{rf}}}, C_{Y_{\delta_{lf}}}$	:	Y-force aerodynamic derivatives due to $\delta_{rf}$ and $\delta_{lf}$
$C_{Z_q}, C_{Z_{\delta_e}}, C_{Z_{\delta_{ra}}}$	:	Z-force aerodynamic derivatives due to $q$ , $\delta_e$ , and $\delta_{ra}$
$C_{Z_{\delta_{la}}}, C_{Z_{\delta_{rf}}}, C_{Z_{\delta_{lf}}}$	:	Z-force aerodynamic derivatives due to $\delta_{la}$ , $\delta_{rf}$ , and $\delta_{lf}$
$C_{l_\beta}, C_{l_p}, C_{l_r}$	:	Roll moment aerodynamic derivatives due to $\beta$ , $p$ , and $r$
$C_{l_{\delta_r}}, C_{l_{\delta_{ra}}}, C_{l_{\delta_{la}}}$	:	Roll moment aerodynamic derivatives due to $\delta_r$ , $\delta_{ra}$ , and $\delta_{la}$
$C_{l_{\delta_{rf}}}, C_{l_{\delta_{lf}}}$	:	Roll moment aerodynamic derivatives due to $\delta_{rf}$ and $\delta_{lf}$
$C_{m_q}, C_{m_{\delta_e}}, C_{m_{\delta_{ra}}}$	:	Pitch moment aerodynamic derivatives due to $q$ , $\delta_e$ , and $\delta_{ra}$
$C_{m_{\delta_{la}}}, C_{m_{\delta_{rf}}}, C_{m_{\delta_{lf}}}$	:	Pitch moment aerodynamic derivatives due to $\delta_{la}$ , $\delta_{rf}$ , and $\delta_{lf}$
$C_{n_\beta}, C_{n_p}, C_{n_r}$	:	Yaw moment aerodynamic derivatives due to $\beta$ , $p$ , and $r$
$C_{n_{\delta_r}}, C_{n_{\delta_{ra}}}, C_{n_{\delta_{la}}}$	:	Yaw moment aerodynamic derivatives due to $\delta_r$ , $\delta_{ra}$ , and $\delta_{la}$
$C_{n_{\delta_{rf}}}, C_{n_{\delta_{lf}}}$	:	Yaw moment aerodynamic derivatives due to $\delta_{rf}$ and $\delta_{lf}$

## 1 INTRODUCTION

Gain-scheduled control techniques have been applied for control of a nonlinear system over decades [22, 28, 12]. One of the gain-scheduled control techniques promising global stability of a controlled system is an LPV control synthesis methodology [2, 6, 32, 25]. An LPV control methodology is also particularly appealing in that robust linear control techniques in an LPV system can be applied to a nonlinear system using well-developed linear robust control concepts [34] without the loss of stability guarantees. To apply an LPV synthesis and analysis methodology to a nonlinear system, it is required that its nonlinearity be represented in the LPV form over the entire operating envelope.

A few studies [2, 30, 24, 13, 15] have been reported considering LPV representations of nonlinear systems. In Refs. [2, 14, 21], an affine-LPV model has been introduced, whose system matrices are affine functions of parameters. To represent nonlinear dynamics as an affine-LPV model, the convex set of a constructed LPV model is generally larger than actual nonlinear dynamics. This may lead to conservative results in control synthesis. An alterna-

tive method of LPV representation is a grid-LPV model whose system matrices are functions of the parameters at all grid points over the entire parameter space [6, 32, 25]. This LPV representation has been used for a grid-LPV synthesis method in which linear matrix inequality constraints are evaluated at all grid points. Generally, there is a trade-off between accuracy in representing the original nonlinear dynamics and computational cost (memory and computational time) for a grid LPV representation method. The grid-LPV representation and control synthesis methods have been used for several control problems: pitch-axis missile autopilots [33, 24], F-14 aircraft lateral-directional axis during powered approach [5, 3], and turbofan engines [31, 4]. In this paper, we will focus on a grid-LPV representation of a nonlinear system since the representation can be applied to a large class of nonlinear systems without the restriction of affine-function dependence of scheduling parameters.

There are a few methods [10, 24, 30] to generate a grid-LPV model from a nonlinear mathematical model. The most common way to generate a grid-LPV model is the first order approximation of a nonlinear system around equilibrium points. This is called the “Jacobian linearization method” which has been used in many applications [10, 20, 25, 15]. As noted in Refs. [10, 20, 25, 15], an LPV model generated by the Jacobian linearization method can capture nonlinear dynamics only around equilibrium points. Another method is a “state transformation” method which has been introduced in Ref. [24]. In this method, state coordinates are changed along with an equilibrium trajectory of scheduling parameters to remove nonlinear dependence on states and inputs of a nonlinear system. The method can generate an accurate LPV model (not using the first order approximation) of a nonlinear system. The disadvantage of the method, however, is that it cannot generate an LPV model outside the equilibrium manifold.

One approach to develop an LPV model over the entire operating envelope including outside the equilibrium manifold has been introduced in Refs.[30, 26, 15]. It is called a “function substitution” method in which a nonlinear mathematical model is replaced by a linear combination of functions of scheduling parameters at all grid points over the entire operating envelope. The linear-combination functions are then reformulated into LPV form. To decompose nonlinear functions, a single reference point (one of the equilibrium points) is used, as shown in Refs.[26, 15]. The LPV model generated by the method in Refs.[26, 15] is strongly dependent on the single reference point. Also, the constructed LPV model may not capture the local stability of the original nonlinear system at an equilibrium point. In this paper, we develop a new function substitution method to remove single reference point dependence on an LPV model and to preserve the local stability of the original nonlinear dynamics, while representing the nonlinear dynamics over the entire operating envelope. To preserve local stability, an LPV representation is formulated as a linear optimization problem which is solved by using the linear matrix inequality (LMI) solver interface “YALMIP” [11].

The remainder of the paper is organized as follows: in Section 2, the class of nonlinear systems and a quasi-LPV model are defined and the preliminary background is explained. In Section 3, the current LPV representation methodologies are described in order to math-

ematically define the problem of interest. In Section 4, a new method is described to resolve the problem. In Section 5, the nonlinear dynamics of FASER is described and the suggested method is applied for constructing an LPV model of the longitudinal/lateral-directional motions of the aircraft. The paper concludes with a brief summary in Section 6.

## 2 PRELIMINARY

### General Nonlinear Aircraft System

In this paper, general aircraft dynamics are represented by the following nonlinear mathematical model.

$$\dot{x} = F(x_1)x + G(x_1)u + h(x_1) \quad (1)$$

with a state vector  $x \in \mathcal{R}^{n_x}$ , and a control vector  $u \in \mathcal{R}^{n_u}$ .  $F(x_1)$ ,  $G(x_1)$ , and  $h(x_1)$  are continuous mapping functions:  $\mathcal{R}^{n_{x_1}} \mapsto \mathcal{R}^{n_x \times n_x}$ ,  $\mathcal{R}^{n_{x_1}} \mapsto \mathcal{R}^{n_x \times n_u}$ , and  $\mathcal{R}^{n_{x_1}} \mapsto \mathcal{R}^{n_x}$ , respectively. In Eq. (1), a state vector  $x$  is written as  $x^T = [x_1^T \quad x_2^T]$ . Note that the subvector  $x_1$  is part of the state vector and also a scheduling parameter vector. Assume that the scheduling parameter variations are in the compact set  $\mathcal{P}$  in  $\mathcal{R}^{n_{x_1}}$ , which is called the operating envelope, hereafter. In the operating envelope, the equilibrium locus is defined as the set of equilibrium points  $(\hat{x}_1, \hat{x}_2, \hat{u})$  such that

$$0 = F(\hat{x}_1) \begin{bmatrix} \hat{x}_1 \\ \hat{x}_2 \end{bmatrix} + G(\hat{x}_1)\hat{u} + h(\hat{x}_1). \quad (2)$$

**Definition 1 (local stability):** *The linearized system of a nonlinear system in Eq.(1) is*

$$\dot{x} = Ax + Bu, \quad (3)$$

where matrices  $A$  and  $B$  are obtained by Jacobian linearization about an equilibrium point. When the real parts of all eigenvalues of  $A$  are negative, the nonlinear system is locally stable about the point.

Even though this is a very common definition, it is described here to emphasize the relation between time responses of a nonlinear system with small perturbations on states and the stability results based on the sign of all eigenvalues. Suppose the linearized system at an equilibrium point indicates stability by definition 1. It is obvious that nonlinear time responses of the system with small perturbations on states with input  $u = \hat{u}$  (equilibrium value) should converge to the equilibrium point. In practice, it is possible to test local stability based on time responses unless the system dynamics are very slow. Note that the local stability applies for the neighborhood of the equilibrium point only. To determine local stability for arbitrary points over the entire envelope, time responses of a nonlinear system are simulated with perturbations on the state. This is referred to in this paper as “extended local stability”, and is defined as follows.

**Definition 2 (extended local stability):** Suppose there exists the set  $\mathcal{E}$  of pre-calculated equilibrium points. Given any point  $\bar{x}_1$  in the operating envelope  $\mathcal{P}$ , there exists an equilibrium point  $\hat{x}_{1r}$  such that

$$\hat{x}_{1r} = \operatorname{argmin}_{\hat{x}_1 \in \mathcal{E}} \|W[\bar{x}_1 - \hat{x}_1]\|, \quad \bar{x}_1 \in \mathcal{P}. \quad (4)$$

where  $W$  is a weighting matrix to compensate physical unit difference of each state. The trajectory of the nonlinear system in Eq. (1) is calculated with the initial condition of  $x(0)^T = [\bar{x}_1^T \quad \hat{x}_{2r}^T]$  and the control input  $u = \hat{u}_r$ . Here, equilibrium values of  $\hat{x}_{2r}$  and  $\hat{u}_r$  are associated with  $\hat{x}_{1r}$ . Suppose there exists small number  $\epsilon$  such that

$$\|x(t) - \begin{bmatrix} \hat{x}_{1r} \\ \hat{x}_{2r} \end{bmatrix}\| < \epsilon, \quad t > T > 0, \quad (5)$$

then, the system is stable with respect to the point  $(\hat{x}_{1r}, \hat{x}_{2r})$  around the neighborhood of the point  $\bar{x}_1$  in the operating envelope.

Note that the extended local stability about a grid point does not represent global stability of the nonlinear system [9] and is also strongly dependent on both  $\hat{x}_{1r}$  and  $\bar{x}_1$ . When the time history of  $x(t)$  converges to another point instead of  $(\hat{x}_{1r}, \hat{x}_{2r})$ , stability is not captured by definition 2. From the extended local stability definition, we can only determine whether the system is stable around the grid point. It is noticed that the minimum solution  $\hat{x}_{1r}$  may not be unique with respect to  $\bar{x}_1$ . This implies that the result of the extended local stability may not be unique.

## 2.1 Quasi-LPV System

In this subsection, a quasi-LPV system is briefly described to carry out the LPV representation of the class of nonlinear systems in Eq. (1). A quasi-LPV system is defined as follows:

**Definition 3 (Quasi-LPV system):** A quasi-LPV system is defined as

$$\begin{bmatrix} \dot{x} \\ y \end{bmatrix} = \begin{bmatrix} A(x_1) & B(x_1) \\ C(x_1) & D(x_1) \end{bmatrix} \begin{bmatrix} x \\ u \end{bmatrix} \quad (6)$$

with states  $x^T = [x_1^T \quad x_2^T]$ . Note that the states  $x_1$  are scheduling parameters whose variations are in the compact set  $\mathcal{P} \in \mathcal{R}^{n_{x_1}}$ .

The detailed description of a quasi-LPV system is available in Refs. [24, 20]. When a quasi-LPV model is used for analysis or control synthesis for a nonlinear system, it is assumed that scheduling parameters can independently vary even though the schedule parameter vector is the part of the state [24, 20].

Stability analysis on a nonlinear system can be formulated into a linear matrix inequality (LMI) optimization using a quasi-LPV representation of the nonlinear model. When a quasi-LPV model in Eq. (6) represents the original nonlinear dynamics, the stability analysis problem is described as follows:

**Lemma 1 (global stability) [6]** *Suppose there exists a positive definite matrix  $P$  such that*

$$A^T(x_1)P + PA(x_1) < 0, \quad \forall x_1 \in \mathcal{P}. \quad (7)$$

*Then, the system is globally stable over the operating envelope  $\mathcal{P}$ .*

This is easily proved using Lyapunov function  $V = x^T P x$ . In practice, the LMI constraints in Eq. (7) are evaluated in all grid points over the envelope  $\mathcal{P}$ . Thus, the frozen dynamics at a fixed parameter plays an important role with determining local and global stability of the original nonlinear dynamics.

### 3 PROBLEM STATEMENT

#### 3.1 Set of Linearized Models

Recall that a set of linearized models of a nonlinear system is considered as a quasi-LPV model for the control synthesis [25]. One approach to construct a linearized model set is to linearize a nonlinear system about equilibrium points using a Jacobian linearization method. The set  $\mathcal{M}_{JL}$  of linearized models of a nonlinear system Eq.(1) is

$$\mathcal{M}_{JL} \equiv \left\{ \dot{\tilde{x}} = \left( \frac{\partial(F(x_1)x)}{\partial x} \Big|_{\hat{x}} + \frac{\partial G(x_1)u}{\partial x} \Big|_{\hat{x}, \hat{u}} + \frac{\partial h(x_1)}{\partial x} \Big|_{\hat{x}} \right) \tilde{x} + G(\hat{x}_1) \tilde{u} : \tilde{x} = x - \hat{x}, \tilde{u} = u - \hat{u} \right\} \quad (8)$$

where  $(\hat{x}, \hat{u})$  is an equilibrium point. When scheduling parameters  $\hat{x}_1$  are chosen along the locus of equilibrium points,  $\hat{x}_2$  and  $\hat{u}$  are associated with  $\hat{x}_1$ . Then the set of linearized models can be written in a quasi-LPV form:

$$\dot{\tilde{x}} = A(\tilde{x}_1) \tilde{x} + B(\tilde{x}_1) \tilde{u} \quad (9)$$

where

$$\begin{aligned} A(\tilde{x}_1) &= \frac{\partial(F(x_1)x)}{\partial x} \Big|_{\hat{x}} + \frac{\partial G(x_1)u}{\partial x} \Big|_{\hat{x}, \hat{u}} + \frac{\partial h(x_1)}{\partial x} \Big|_{\hat{x}}, \\ B(\tilde{x}_1) &= G(\hat{x}_1). \end{aligned}$$

Note that this quasi-LPV model is a collection of linearized dynamic systems around the equilibrium points/trajectory [13] since the state and input definitions are changed according to an equilibrium point associated with the current scheduling parameters  $(\hat{x}_1)$ . Advantages of this well-known method are: 1) applicable to a wide-class of nonlinear systems without restriction of affine dependence of input  $u$  on a nonlinear system, and 2) able to represent local stability of the nonlinear system preserving the stability of a quasi-LPV system at “frozen” parameters described in Lemma 1.

The quasi-LPV model constructed by this method can represent the true nonlinear dynamics at the neighborhood of equilibrium points only. Choosing the number of grid points along the locus of equilibrium points also plays an important role in the representation of the nonlinear dynamics. The optimal way to choose grid points is still unknown.

### 3.2 Function Substitution Quasi-LPV Model

The function substitution method has been introduced in Refs.[30, 25, 15] to construct a quasi-LPV model over the entire operating region, including a non-trim region. To perform the substitution method, choose an equilibrium point as a reference point  $(x_{1r}, x_{2r}, u_r)$  and transform the states into

$$\tilde{x}_1 = x_1 - x_{1r}, \quad \tilde{x}_2 = x_2 - x_{2r}, \quad \tilde{u} = u - u_r. \quad (10)$$

Using Eq. (10), the nonlinear system of Eq. (1) can be rewritten as

$$\begin{bmatrix} \dot{\tilde{x}}_1 \\ \dot{\tilde{x}}_2 \end{bmatrix} = \begin{bmatrix} A_{11}(x_1) & A_{12}(x_1) \\ A_{21}(x_1) & A_{22}(x_1) \end{bmatrix} \begin{bmatrix} \tilde{x}_1 \\ \tilde{x}_2 \end{bmatrix} + \begin{bmatrix} B_1(x_1) \\ B_2(x_1) \end{bmatrix} \tilde{u} + f(x_1) \quad (11)$$

where

$$f(x_1) = \begin{bmatrix} A_{11}(x_1) & A_{12}(x_1) \\ A_{21}(x_1) & A_{22}(x_1) \end{bmatrix} \begin{bmatrix} x_{1r} \\ x_{2r} \end{bmatrix} + \begin{bmatrix} B_1(x_1) \\ B_2(x_1) \end{bmatrix} u_r + h(x_1). \quad (12)$$

The main goal of this method is to reformulate the function  $f(x_1)$  in Eq.(12) into quasi-LPV functional form such that

$$f(x_1) = E(x_1)\tilde{x}_1 = \begin{bmatrix} e_{1.}(x_1) \\ \vdots \\ e_{n.}(x_1) \end{bmatrix} \tilde{x}_1 \quad (13)$$

where the matrix  $E$  is an unknown matrix to be determined and  $e_i$  is the  $i$ -th row vector of the matrix  $E$ . There are infinite numbers of possible solutions to Eq. (13) since this is an under-determined problem. In Refs.[25, 15], the matrix  $E$  is calculated to minimize the variations of each matrix element over the entire operating envelope.

The final quasi-LPV form of the nonlinear system is

$$\begin{bmatrix} \dot{\tilde{x}}_1 \\ \dot{\tilde{x}}_2 \end{bmatrix} = A_f \begin{bmatrix} \tilde{x}_1 \\ \tilde{x}_2 \end{bmatrix} + \begin{bmatrix} B_1(x_1) \\ B_2(x_1) \end{bmatrix} \tilde{u}. \quad (14)$$

where

$$A_f = \begin{bmatrix} A_{11}(x_1) & A_{12}(x_1) \\ A_{21}(x_1) & A_{22}(x_1) \end{bmatrix} + [E \mid 0_{n \times n_{x_2}}]. \quad (15)$$

The solution of the quasi-LPV system is close to the solution of the nonlinear system since the equality constraint in Eq. (13) is satisfied at all grid points. This is a strong advantage of this method.

This method, however, has disadvantages such as 1) a strong dependence of the quasi-LPV model on the reference point and 2) possible misrepresentation of local stability of the original nonlinear system over the locus of equilibrium points. The matrix  $A_f$  of the quasi-LPV model can change when a different equilibrium point is chosen as a reference point. The stability analysis described in Lemma 1 may fail even though the original nonlinear dynamics are exponentially stable. Since all LMI constraints in Lemma 1 are evaluated at all grid points, the matrix  $A_f$  at each grid point must be stable to represent the stable nonlinear dynamics. The current limitations of the method in Refs.[26, 15] are choosing the correct reference point and representing the local stability of the original nonlinear system at a grid point. In the next section, the limitations will be relaxed by a new function substitution method.

#### 4 QUASI-LPV REPRESENTATION DEVELOPMENT

A new method is described in this paper to construct a quasi-LPV model of a nonlinear system over the entire operating envelope including a non-trim region. The model can also capture the local stability of the original nonlinear system. In the new method, many reference points are chosen along the locus of equilibrium points to preserve the local stability of the system. The details are described in the four step process below:

First, grid points are generated over the entire operating envelope  $\mathcal{P}$  and each grid point is assigned with its own reference point. This allows us to reformulate the nonlinear function  $f(x_1)$  in Eq.(12) into quasi-LPV form. A reference point for each grid point is determined by Eq. (4).

Second,  $E$  in Eq. (13) is written in terms of the variables  $\phi_i$  to satisfy the equality constraint. When a grid point  $\bar{x}_1$  is not equal to a reference point  $x_{1r}$ , Eq. (13) is rewritten as:

$$\begin{bmatrix} f_1(\bar{x}_1) \\ \vdots \\ f_n(\bar{x}_1) \end{bmatrix} = \begin{bmatrix} [\bar{x}_1 - x_{1r}]^T e_1^T \\ \vdots \\ [\bar{x}_1 - x_{1r}]^T e_n^T \end{bmatrix}. \quad (16)$$

The possible solutions of  $e_i^T$  in Eq. (16) can be written as

$$e_i^T = e_{i,p}^T + \mathcal{N}([\bar{x}_1 - x_{1r}]^T) \phi_i \quad (17)$$

where the particular solution  $e_{i,p}^T$  is

$$e_{i,p}^T = [\bar{x}_1 - x_{1r}]([\bar{x}_1 - x_{1r}]^T[\bar{x}_1 - x_{1r}])^{-1} f_i, \quad (18)$$

$\mathcal{N}([\bar{x}_1 - x_{1r}]^T)$  is the null space of  $[\bar{x}_1 - x_{1r}]^T$ , and  $\phi_i$  is a unknown vector associated with the null space dimension. Using Eq. (17), the matrix  $A_f$  is rewritten as:

$$A_f = A_p + [\Phi^T \mathcal{N}^T([\bar{x}_1 - x_{1r}]^T) \mid 0_{n \times n_{x_2}}] \quad (19)$$

where

$$A_p = \begin{bmatrix} A_{11} & A_{12} \\ A_{21} & A_{22} \end{bmatrix} + [E_p \mid 0_{n \times n_{x_2}}], \quad (20)$$

the matrix  $E_p$  is the collection of  $e_{i,p}^T$  and the matrix  $\Phi$  is the collection of  $\phi_i$ .

When a grid point is equal to a reference point  $x_{1r}$ , notice that  $f(\bar{x}_1)$  and  $\dot{\bar{x}}_1$  are zero. The particular solution of Eq. (18) cannot be defined since it is a singular point. For this case, the matrix  $E$  defined in Eq. (13) is defined as

$$E = \lim_{\bar{x}_1 \rightarrow x_{1r}} \frac{f(\bar{x}_1)}{\bar{x}_1 - x_{1r}}. \quad (21)$$

Using Eqs. (15) and (21), the matrix  $A_f$  is calculated for a quasi-LPV model at the grid point. Noticed that the calculated  $A_f$  is exactly the same as the matrix  $A$  obtained by Jacobian linearization at the grid point. This is proved after algebraic manipulations with Eqs. (11) and (12).

Third, a linear matrix inequality is constructed to represent stability of the original nonlinear dynamics with prior information of the extended local stability of the system at every grid point. When the original nonlinear system is stable, the following LMI must be satisfied for all grid points.

$$(A_p + [\Phi^T \mathcal{N}^T \mid 0_{n \times n_{x_2}}])^T P + P(A_p + [\Phi^T \mathcal{N}^T \mid 0_{n \times n_{x_2}}]) < 0, \quad P > 0, \quad x_1 \in \mathcal{P} \quad (22)$$

where  $P$  is a constant positive matrix. Note that Eq. (22) has unknowns  $P$  and  $\Phi$  in multiple form. This makes the LMI constraints not convex in  $P$  and  $\Phi$ . It is a bilinear matrix inequality (BMI) problem. Generally, it is hard to find a global solution to a BMI problem. In this paper, the feasible solution of  $\Phi$  is calculated using the Ruth-Hurwitz condition. Then, the LMI optimization Eq. (22) is solvable with the calculated feasible solution  $\Phi$ . The detailed method is described in the next section.

Fourth, for smoothness of the matrix  $A_f$  elements, a linear optimization problem is formulated to penalize the derivatives of the matrix elements due to  $x_1$ . The details of constructing a linear optimization problem is described in the next section.

## 5 EXAMPLE

In this section, it is demonstrated how to construct a quasi-LPV model using the proposed method. The nonlinear dynamics of FASER are represented by a quasi-LPV model. FASER (see Fig. 1), developed at NASA Langley Research Center, has conventional high wing and tail configuration with 7 ft wingspan [17]. The detailed shape and physical quantities are available in Refs.[16, 17].

## 5.1 Nonlinear Equations of Motion

In this subsection, general nonlinear equations of aircraft motion [7] are reformulated into matrix form described in Eq. (1).

Force equations of an aircraft are

$$\dot{u} = rV \sin \beta - qV \sin \alpha \cos \beta - g \sin \theta + \frac{\bar{q}SC_X + T}{m} \quad (23)$$

$$\dot{v} = pV \sin \alpha \cos \beta - rV \cos \alpha \cos \beta + g \cos \theta \sin \phi + \frac{\bar{q}SC_Y}{m} \quad (24)$$

$$\dot{w} = qV \cos \alpha \cos \beta - pV \sin \beta + g \cos \theta \cos \phi + \frac{\bar{q}SC_Z}{m} \quad (25)$$

Kinematic equations of position angles are

$$\dot{\phi} = p + (q \sin \phi + r \cos \phi) \tan \theta \quad (26)$$

$$\dot{\theta} = q \cos \phi - r \sin \phi \quad (27)$$

$$\dot{\psi} = (q \sin \phi + r \cos \phi) / \cos \theta \quad (28)$$

and moment equations are

$$\begin{bmatrix} \dot{p} \\ \dot{q} \\ \dot{r} \end{bmatrix} = J^{-1} \begin{bmatrix} L \\ M \\ N \end{bmatrix} + J^{-1} \begin{bmatrix} J_{zx}q - J_{xy}r & J_{yz}q - J_{zz}r & J_{yy}q - J_{yz}r \\ J_{zz}r - J_{zx}p & J_{xy}r - J_{yz}p & J_{zx}r - J_{xx}p \\ J_{xy}p - J_{yy}q & J_{xx}p - J_{xy}q & J_{yz}p - J_{zx}q \end{bmatrix} \begin{bmatrix} p \\ q \\ r \end{bmatrix} \quad (29)$$

where the inverse of the inertial moment  $J$  is

$$J^{-1} = \frac{1}{J_D} \begin{bmatrix} J_{yy}J_{zz} - J_{yz}^2 & J_{xz}J_{yz} + J_{zz}J_{xy} & J_{xy}J_{yz} + J_{xz}J_{yy} \\ J_{xy}J_{zz} + J_{xz}J_{yz} & J_{xx}J_{zz} - J_{xz}^2 & J_{xx}J_{yz} + J_{xy}J_{xz} \\ J_{xy}J_{yz} + J_{xz}J_{yy} & J_{xx}J_{yz} + J_{xy}J_{xz} & J_{xx}J_{yy} - J_{xy}^2 \end{bmatrix} \quad (30)$$

and the scalar  $J_D$  is

$$J_D = J_{xx}J_{yy}J_{zz} - J_{xx}J_{yz}^2 - J_{zz}J_{xy}^2 - 2J_{xy}J_{xz}J_{yz} - J_{yy}J_{xz}^2. \quad (31)$$

The roll, pitch and yaw moments ( $L$ ,  $M$ ,  $N$ ) are functions of dynamic pressure  $\bar{q}$ , reference area  $S$ , wing span  $b$ , mean chord length  $\bar{c}$ , and moment aerodynamic coefficients  $C_l$ ,  $C_m$  and  $C_n$ .

$$L = \bar{q}SbC_l, \quad M = \bar{q}S\bar{c}C_m, \quad N = \bar{q}SbC_n \quad (32)$$

After simple algebraic manipulation of Eqs. (23)-(25), the force equations in Eqs. (23)-(25) can be rewritten in terms of total velocity  $V$ , angle of attack  $\alpha$ , and side-slip angle  $\beta$ . This

leads to

$$\begin{aligned}\dot{V} = & \frac{1}{m} \{ (\bar{q}SC_x + T) \cos \alpha \cos \beta + \bar{q}SC_Y \sin \beta + \bar{q}SC_Z \sin \alpha \cos \beta \} \\ & + g(\cos \theta \sin \phi \sin \beta - \sin \theta \cos \alpha \cos \beta + \cos \theta \cos \phi \sin \alpha \cos \beta)\end{aligned}\quad (33)$$

$$\begin{aligned}\dot{\alpha} = & q - \frac{\cos \alpha \sin \beta}{\cos \beta} p - \frac{\sin \alpha \sin \beta}{\cos \beta} r + \frac{\bar{q}SC_Z \cos \alpha}{mV \cos \beta} - \frac{\bar{q}SC_X + T}{mV_t \cos \beta} \sin \alpha \\ & + \frac{g}{V \cos \beta} (\cos \alpha \cos \theta \cos \phi + \sin \theta \sin \alpha)\end{aligned}\quad (34)$$

$$\begin{aligned}\dot{\beta} = & p \sin \alpha - r \cos \alpha + \frac{\bar{q}SC_Y}{mV_t} \cos \beta - \frac{\bar{q}SC_X + T}{mV_t} \cos \alpha \sin \beta - \frac{\bar{q}SC_Z}{mV_t} \sin \beta \sin \alpha \\ & + \frac{g}{V_t} (\cos \theta \sin \phi \cos \beta + \sin \beta \cos \theta \cos \alpha - \cos \theta \cos \phi \sin \alpha \sin \beta).\end{aligned}\quad (35)$$

From Eqs.(33)-(35), (26)-(29) notice that the states are  $V$ ,  $\alpha$ ,  $\beta$ , body angular rates  $p$ ,  $q$ ,  $r$ , and position angles  $\phi$ ,  $\theta$ , and  $\psi$  for the nonlinear dynamics.

## 5.2 Aerodynamic Coefficients

Force and moment equations in Eqs. (23)-(25), (29) are dependent on aerodynamic coefficients  $C_X$ ,  $C_Y$ ,  $C_Z$ ,  $C_l$ ,  $C_m$ , and  $C_n$ . In this example, the aerodynamic coefficients are functions of angle of attack, and control surface deflections such as elevator deflection  $\delta_e$  (deg), right aileron deflection  $\delta_{ra}$  (deg), left aileron deflection  $\delta_{la}$  (deg), right flap deflection  $\delta_{rf}$  (deg), left flap deflection  $\delta_{lf}$  (deg), and rudder deflection  $\delta_r$  (deg). The aerodynamic coefficients are

$$\begin{aligned}C_X = & C_{X_o}(\alpha) + C_{X_q}(\alpha) \frac{\bar{c}}{2V} q + C_{X_{\delta_e}}(\alpha) \delta_e + C_{X_{\delta_{ra}}}(\alpha) \delta_{ra} + C_{X_{\delta_{la}}}(\alpha) \delta_{la} \\ & + C_{X_{\delta_{rf}}}(\alpha) \delta_{rf} + C_{X_{\delta_{lf}}}(\alpha) \delta_{lf}\end{aligned}\quad (36)$$

$$\begin{aligned}C_Y = & C_{Y_\beta}(\alpha) \beta + \frac{b}{2V} (C_{Y_p}(\alpha) p + C_{Y_r}(\alpha) r) + C_{Y_{\delta_r}}(\alpha) \delta_r + C_{Y_{\delta_{ra}}}(\alpha) \delta_{ra} + C_{Y_{\delta_{la}}}(\alpha) \delta_{la} \\ & + C_{Y_{\delta_{rf}}}(\alpha) \delta_{rf} + C_{Y_{\delta_{lf}}}(\alpha) \delta_{lf}\end{aligned}\quad (37)$$

$$\begin{aligned}C_Z = & C_{Z_o}(\alpha) + C_{Z_q}(\alpha) \frac{\bar{c}}{2V} q + C_{Z_{\delta_e}}(\alpha) \delta_e + C_{Z_{\delta_{ra}}}(\alpha) \delta_{ra} + C_{Z_{\delta_{la}}}(\alpha) \delta_{la} \\ & + C_{Z_{\delta_{rf}}}(\alpha) \delta_{rf} + C_{Z_{\delta_{lf}}}(\alpha) \delta_{lf}\end{aligned}\quad (38)$$

$$C_l = C_{l_\beta}(\alpha)\beta + \frac{b}{2V}(C_{l_p}(\alpha)p + C_{l_r}(\alpha)r) + C_{l_{\delta_r}}(\alpha)\delta_r + C_{l_{\delta_{ra}}}(\alpha)\delta_{ra} + C_{l_{\delta_{la}}}(\alpha)\delta_{la} \\ + C_{l_{\delta_{rf}}}(\alpha)\delta_{rf} + C_{l_{\delta_{lf}}}(\alpha)\delta_{lf} \quad (39)$$

$$C_m = C_{m_o}(\alpha) + C_{m_q}(\alpha)\frac{\bar{c}}{2V}q + C_{m_{\delta_e}}(\alpha)\delta_e + C_{m_{\delta_{ra}}}(\alpha)\delta_{ra} + C_{m_{\delta_{la}}}(\alpha)\delta_{la} \\ + C_{m_{\delta_{rf}}}(\alpha)\delta_{rf} + C_{m_{\delta_{lf}}}(\alpha)\delta_{lf} \quad (40)$$

$$C_n = C_{n_\beta}(\alpha)\beta + \frac{b}{2V}(C_{n_p}(\alpha)p + C_{n_r}(\alpha)r) + C_{n_{\delta_r}}(\alpha)\delta_r + C_{n_{\delta_{ra}}}(\alpha)\delta_{ra} + C_{n_{\delta_{la}}}(\alpha)\delta_{la} \\ + C_{n_{\delta_{rf}}}(\alpha)\delta_{rf} + C_{n_{\delta_{lf}}}(\alpha)\delta_{lf} \quad (41)$$

The aerodynamic coefficients  $C_{X_o}$ ,  $C_{Z_o}$ , and  $C_{m_o}$  and aerodynamic derivatives are functions of angle of attack and were calculated by Paul Chwalowski[19] using CMARC [1] and VORVIEW [8, 27]. The CMARC is a commercial version of potential flow method developed at NASA Ames. The calculated aerodynamic coefficients are compared with the results of wind tunnel experiments[17] done at the NASA Langley 12-foot Low Speed Wind Tunnel. In this paper, the calculated aerodynamic coefficients are used to develop a quasi-LPV model of the aircraft since the comparison results [19] show that the CFD calculation accurately predicts the aerodynamic coefficients of the FASER aircraft.

### 5.3 Reformulated Nonlinear Equations of Motion

In this subsection, the nonlinear equations described in the previous section are written in matrix form of Eq. (1) to formulate quasi-LPV representation.

When states  $X_{st} = [V \ \alpha \ \beta \ p \ q \ r \ \theta \ \phi]^T$  and controls  $U = [T \ \delta_e \ \delta_{ra} \ \delta_{la} \ \delta_{rf} \ \delta_{lf} \ \delta_r]^T$ , the nonlinear equations of motion can be rewritten as

$$\dot{X}_{st} = A(V, \alpha, \beta, p, q, r, \theta, \phi)X_{st} + B(V, \alpha, \beta)U + h(V, \alpha, \beta) \quad (42)$$

where the detailed elements of the matrices  $A$ ,  $B$ , and  $h$  are written in Appendix A.

Note that it is possible to generate a quasi-LPV model for the full 6 DOF motion but scheduling parameters in a quasi-LPV model would be all states. When all states are scheduling parameters, a quasi-LPV model can lead very conservative results in control synthesis since scheduling parameters are considered independent on each other in LPV control synthesis [29, 23].

To generate a practically useful quasi-LPV model for control synthesis, the nonlinear dynamics are decoupled into the longitudinal motion and the lateral-directional motion. For the longitudinal motion of the aircraft, state  $X_{lon}$  is set as  $X_{lon} = [V \ \alpha \ q \ \theta]^T$  and control  $U_{lon}$  is set as  $U_{lon} = [T \ \delta_e \ \delta_{a_s} \ \delta_{f_s}]^T$ , where  $\delta_{a_s} \equiv 0.5(\delta_{ra} + \delta_{la})$  and  $\delta_{f_s} \equiv 0.5(\delta_{rf} + \delta_{lf})$ . Positive deflection of all control surfaces except the rudder is defined as trailing edge down. For control of the longitudinal motion, the right/left ailerons are assumed to

move symmetrically and so do the right/left flaps. Since the other variables are set as zero for the longitudinal motion, the nonlinear equation of longitudinal motion is

$$\dot{X}_{lon} = A_{lon}(V, \alpha)X_{lon} + B_{lon}(V, \alpha)U_{lon} + h_{lon}(V, \alpha), \quad (43)$$

where the elements of the matrices  $A_{lon}$ ,  $B_{lon}$ , and  $h_{lon}$  are given in Appendix B.

For lateral-directional motion, the states are  $X_{lat} = [\beta \ p \ r \ \phi]^T$  and the controls are  $U_{lat} = [\delta_{aas} \ \delta_{fas} \ \delta_r]^T$ , where  $\delta_{aas} \equiv 0.5(\delta_{la} - \delta_{ra})$  and  $\delta_{fas} \equiv 0.5(\delta_{lf} - \delta_{rf})$ . The right and left ailerons are assumed to move asymmetrically for control of lateral-directional motion. The nonlinear equations of lateral-directional motion is

$$\dot{X}_{lat} = A_{lat}(V, \alpha, \beta, \phi)X_{lat} + B_{lat}(V, \alpha)U_{lat} \quad (44)$$

where the elements of the matrices  $A_{lat}$  and  $B_{lat}$  are given in Appendix B. From Eq. (44), notice that the matrix form of the lateral-directional motion is already in quasi-LPV form with exogenous scheduling parameters  $V$  and  $\alpha$  and state-scheduling parameter  $\beta$  and  $\phi$ .

#### 5.4 Quasi-LPV Model of Longitudinal Motion

To construct a quasi-LPV model of the longitudinal motion by using the new method, the locus of equilibrium points is calculated over the flight envelope defined as

$$50 \leq V \leq 200 \text{ ft/s}, \quad 0.5 \leq \alpha \leq 10 \text{ deg}. \quad (45)$$

The chosen equilibrium points are numbered as shown in Fig. 2 while the grid points are defined as shown in Fig. 2. Using Eq. (4), every grid point is assigned to an equilibrium point. The assigned equilibrium point is called a reference point for the grid point.

To apply the method, the stability information of the nonlinear longitudinal dynamics is required. The local stability of the motion around equilibrium point is easily tested by checking eigenvalues of the matrix  $A$  obtained by the Jacobian linearization method. The extended local stability at every grid point can be tested by using nonlinear simulations at the initial values of  $(\bar{x}_1, \hat{x}_2)$  using the constant input associated with the reference point. Based on the stability test results, we conclude that the longitudinal dynamics are stable for all the grid points.

Now, the decomposed function  $f(x_1)$  of Eq. (12) is evaluated at the grid point  $\bar{x}_1$  using Eq. (17), the particular solutions are calculated at all grid points except the equilibrium points. Note that the matrix  $A_f$  of the quasi-LPV model at the numbered equilibrium points is calculated by using the Jacobian linearization method. It is required to find feasible solutions of  $\Phi^T$  at a grid point to solve the BMI problem. We first try to find the feasible solution by assigning  $\Phi^T$  as a zero matrix. Note that the particular solution of  $A_p$  in Eq. (20) can be the system matrix of a quasi-LPV model. The eigenvalues of the matrix  $A_p$  at every grid point are shown in the left plot of Fig. 3. It is observed from Fig. 3 that there are

unstable eigenvalues of  $A_p$  at some grid points. Thus, this solution is not appropriate to represent the stable nonlinear dynamics of FASER.

Since the matrix  $A_f$  in Eq. (19) can be explicitly written as  $\Phi^T$ , the Ruth-Hurwitz stability [18] of the 4th-order polynomial can be used to find feasible solutions of  $\Phi^T$ . The stability conditions of the 4th-order polynomial  $s^4 + \tilde{a}s^3 + \tilde{b}s^2 + \tilde{c}s + \tilde{d}$  are  $\tilde{a} > 0$ ,  $\tilde{b} > 0$ ,  $\tilde{c} > 0$ ,  $\tilde{d} > 0$ ,  $\tilde{a}\tilde{b} > \tilde{c}$  and  $\tilde{a}\tilde{b}\tilde{c} - \tilde{c}^2 > \tilde{d}\tilde{a}^2$ . To use the stability condition, the matrix  $A_f$  is rewritten as:

$$A_f(V, \alpha) = \begin{bmatrix} a_{11}^p(V, \alpha) + \phi_1(V, \alpha)n_1(V, \alpha) & a_{12}^p(V, \alpha) + \phi_1(V, \alpha)n_2(V, \alpha) & a_{13}^p(V, \alpha) & a_{14}^p(V, \alpha) \\ a_{21}^p(V, \alpha) + \phi_2(V, \alpha)n_1(V, \alpha) & a_{22}^p(V, \alpha) + \phi_2(V, \alpha)n_2(V, \alpha) & a_{23}^p(V, \alpha) & a_{24}^p(V, \alpha) \\ a_{31}^p(V, \alpha) + \phi_3(V, \alpha)n_1(V, \alpha) & a_{32}^p(V, \alpha) + \phi_3(V, \alpha)n_2(V, \alpha) & a_{33}^p(V, \alpha) & 0 \\ 0 & 0 & 1 & 0 \end{bmatrix} \quad (46)$$

where  $\phi_1$ ,  $\phi_2$ , and  $\phi_3$  are unknown parameters to be determined,  $n_1$  and  $n_2$  are the elements of the null space and  $a_{ij}^p$  is the element of the matrix  $A_p$ . For convenience, the dependence of  $V$  and  $\alpha$  on parameters is omitted hereafter.

After some algebraic manipulations, the conditions  $\tilde{a} > 0$ ,  $\tilde{b} > 0$ ,  $\tilde{c} > 0$ ,  $\tilde{d} > 0$  can be rewritten as

$$g_a^T x > 0, \quad g_b^T x > 0, \quad g_c^T x > 0, \quad g_d^T x > 0 \quad (47)$$

where  $x^T = [1 \ \phi_1 \ \phi_2 \ \phi_3]$  and the coefficient vectors  $g_a^T$ ,  $g_b^T$ ,  $g_c^T$ , and  $g_d^T$  are written in terms of  $a_{ij}^p$ ,  $n_1$  and  $n_2$ . Here, the detailed expression of the coefficients vectors are in Appendix C. The condition  $\tilde{a}\tilde{b} > \tilde{c}$  is relaxed by the following linear inequalities  $\tilde{a} > 1$ ,  $\tilde{b} > 1$ ,  $\tilde{a} > \tilde{c}$ , and  $\tilde{b} > \tilde{c}$ . The other condition is relaxed by minimizing  $\tilde{d}$  value.

For the smooth variation of each matrix  $A_f$  element due to  $V$  and  $\alpha$  changes, the derivatives of each element with respect to  $V$  and  $\alpha$  are imposed by solving the following optimization problem.

$$\min_{\phi_1, \phi_2, \phi_3} W_t[t \ \epsilon_V \ \epsilon_\alpha]^T \quad (48)$$

subject to

$$\begin{bmatrix} g_a^T \\ g_b^T \\ g_c^T \\ g_d^T \\ g_a^T - g_c^T \\ g_b^T - g_c^T \end{bmatrix} \begin{bmatrix} 1 \\ \phi_1 \\ \phi_2 \\ \phi_3 \end{bmatrix} - \begin{bmatrix} 1 \\ 1 \\ 0 \\ 0 \\ 0 \\ 0 \end{bmatrix} > 0, \quad [1 \ \phi_1 \ \phi_2 \ \phi_3]g_d < t, \quad (49)$$

$$\begin{aligned}
\left| \frac{\partial(a_{11}^p + \phi_1 n_1)}{\partial V} \right| < \epsilon_{V_1}, & \quad \left| \frac{\partial(a_{11}^p + \phi_1 n_1)}{\partial \alpha} \right| < \epsilon_{\alpha_1} \\
\left| \frac{\partial(a_{12}^p + \phi_1 n_2)}{\partial V} \right| < \epsilon_{V_2}, & \quad \left| \frac{\partial(a_{12}^p + \phi_1 n_2)}{\partial \alpha} \right| < \epsilon_{\alpha_2} \\
\left| \frac{\partial(a_{21}^p + \phi_2 n_1)}{\partial V} \right| < \epsilon_{V_3}, & \quad \left| \frac{\partial(a_{21}^p + \phi_2 n_1)}{\partial \alpha} \right| < \epsilon_{\alpha_3} \\
\left| \frac{\partial(a_{22}^p + \phi_2 n_2)}{\partial V} \right| < \epsilon_{V_4}, & \quad \left| \frac{\partial(a_{22}^p + \phi_2 n_2)}{\partial \alpha} \right| < \epsilon_{\alpha_4} \\
\left| \frac{\partial(a_{31}^p + \phi_3 n_1)}{\partial V} \right| < \epsilon_{V_5}, & \quad \left| \frac{\partial(a_{31}^p + \phi_3 n_1)}{\partial \alpha} \right| < \epsilon_{\alpha_5} \\
\left| \frac{\partial(a_{32}^p + \phi_3 n_2)}{\partial V} \right| < \epsilon_{V_6}, & \quad \left| \frac{\partial(a_{32}^p + \phi_3 n_2)}{\partial \alpha} \right| < \epsilon_{\alpha_6}
\end{aligned} \tag{50}$$

where  $W_t$  is a constant weighting vector to scale the parameter  $t$ ,  $\epsilon_V$ , and  $\epsilon_\alpha$ . The derivatives are calculated using the first order finite differential method between grid points.

After solving the optimization problem using the LMI solver ‘yalmip’ [11], the eigenvalues of the matrix  $A_f$  at every grid point are shown in the right plot of Fig. 3. In Fig. 4 variation of  $a_{11}$  of the matrix  $A_f$  due to  $V$  and  $\alpha$  is shown to verify the smoothness of the solution as compared to the particular solution calculated.

For comparison of the nonlinear dynamics and the generated quasi-LPV model, the dynamics are simulated for the initial condition  $[V \ \alpha \ q \ \theta] = [67 \ 6 \ 0 \ 6]$ , with control action changes such as the thrust doublet and the up-and-down elevator changes, respectively. The simulations results and the control command history are shown in Figs. 5 and 6. Note that the generated quasi-LPV model captures the time history of the original nonlinear dynamics.

## 6 CONCLUSION

In this paper, a new quasi-LPV representation method is proposed to reformulate a nonlinear mathematical model into a quasi-LPV form. The suggested method preserves the local and global stability of the original nonlinear system over the entire parameter space including the non-trim region. Nonlinear equations of motion for a general aircraft are formulated into matrix form which can be converted into quasi-LPV model using this method. For practical use of quasi-LPV models, the nonlinear equations of motion are generally decoupled into the longitudinal and lateral-directional motions. The quasi-LPV representation of the longitudinal motion for the FASER aircraft has been developed, which has scheduling parameters: velocity and angle of attack. The lateral-directional motion for the aircraft is also modeled as quasi-LPV representation with exogenous scheduling parameters  $V$  and  $\alpha$  and state-scheduling parameters  $\beta$  and  $\phi$ . It has been shown that the longitudinal motion represented by the quasi-LPV model preserves the stability of the original nonlinear dynamics at every grid point and represents the nonlinear dynamics over the entire parameter space.

## APPENDIX A

### Matrix Form of Nonlinear Equation of Aircraft Motion

After substitution of aerodynamic coefficients of Eqs. (36)-(41) into nonlinear force equations in Eqs.(33)-(35), the force equations are rewritten as

$$\begin{bmatrix} \dot{V} \\ \dot{\alpha} \\ \dot{\beta} \end{bmatrix} = A_{force}[V \ \alpha \ \beta \ p \ q \ r]^T + B_{force}[T \ \delta_e \ \delta_{ra} \ \delta_{la} \ \delta_{rf} \ \delta_{lf} \ \delta_r]^T + h_{force} \quad (51)$$

where

$$A_{force} = \begin{bmatrix} 0 & 0 & \frac{\bar{q}SS\beta C_{Y\beta}}{m} & \frac{\bar{q}SbS\beta C_{Yp}}{2mV} & \frac{\bar{q}S\bar{c}C\beta}{2mV}(C_{Xq}C_\alpha + C_{Zq}S_\alpha) & \frac{\bar{q}SbS\beta C_{Yr}}{2mV} \\ 0 & 0 & 0 & -\frac{C_\alpha S_\beta}{C_\beta} & 1 + \frac{\bar{q}S\bar{c}}{2mV^2 C_\beta}(C_{Zq}C_\alpha - C_{Xq}S_\alpha) & -\frac{S_\alpha S_\beta}{C_\beta} \\ 0 & 0 & \frac{\bar{q}SC\beta C_{Y\beta}}{mV} & S_\alpha + \frac{\bar{q}SbC\beta}{2mV^2}C_{Yp} & -\frac{\bar{q}SS\beta\bar{c}}{2mV^2}(C_{Xq}C_\alpha + C_{Zq}S_\alpha) & -C_\alpha + \frac{\bar{q}SbC\beta}{2mV^2}C_{Yr} \end{bmatrix} \quad (52)$$

$$B_{force} = \begin{bmatrix} B_{f1} & B_{f2} & B_{f3} \end{bmatrix} \quad (53)$$

$$B_{f1} = \begin{bmatrix} \frac{C_\alpha C_\beta}{m} & \frac{\bar{q}SC\beta}{m}(C_{X\delta_e}C_\alpha + C_{Z\delta_e}S_\alpha) \\ -\frac{S_\alpha}{mVC_\beta} & \frac{\bar{q}S}{mVC_\beta}(C_{Z\delta_e}C_\alpha - C_{X\delta_e}S_\alpha) \\ -\frac{C_\alpha S_\beta}{mV} & -\frac{\bar{q}SS\beta}{mV}(C_{X\delta_e}C_\alpha + C_{Z\delta_e}S_\alpha) \end{bmatrix} \quad (54)$$

$$B_{f2} = \frac{\bar{q}S}{mV} \begin{bmatrix} C_\beta V(C_{X\delta_{ra}}C_\alpha + C_{Z\delta_{ra}}S_\alpha) + S_\beta VC_{Y\delta_{ra}} & C_\beta V(C_{X\delta_{la}}C_\alpha + C_{Z\delta_{la}}S_\alpha) + S_\beta VC_{Y\delta_{ra}} \\ (C_{Z\delta_{ra}}C_\alpha - C_{X\delta_{ra}}S_\alpha)/C_\beta & (C_{Z\delta_{la}}C_\alpha - C_{X\delta_{la}}S_\alpha)/C_\beta \\ C_\beta C_{Y\delta_{ra}} - C_\alpha S_\beta C_{X\delta_{ra}} - S_\beta S_\alpha C_{Z\delta_{ra}} & C_\beta C_{Y\delta_{la}} - C_\alpha S_\beta C_{X\delta_{la}} - S_\beta S_\alpha C_{Z\delta_{la}} \end{bmatrix} \quad (55)$$

$$B_{f3} = \frac{\bar{q}S}{mV} \begin{bmatrix} C_\beta V(C_{X\delta_{rf}}C_\alpha + C_{Z\delta_{rf}}S_\alpha) + S_\beta VC_{Y\delta_{rf}} & C_\beta V(C_{X\delta_{lf}}C_\alpha + C_{Z\delta_{lf}}S_\alpha) + S_\beta VC_{Y\delta_{lf}} & S_\beta VC_{Y\delta_r} \\ (C_{Z\delta_{rf}}C_\alpha - C_{X\delta_{rf}}S_\alpha)/C_\beta & (C_{Z\delta_{lf}}C_\alpha - C_{X\delta_{lf}}S_\alpha)/C_\beta & 0 \\ C_\beta C_{Y\delta_{rf}} - C_\alpha S_\beta C_{X\delta_{rf}} - C_{Z\delta_{rf}}S_\beta S_\alpha & C_\beta C_{Y\delta_{lf}} - C_\alpha S_\beta C_{X\delta_{lf}} - C_{Z\delta_{lf}}S_\beta S_\alpha & C_{Y\delta_r}C_\beta \end{bmatrix} \quad (56)$$

and

$$h_{force} = \begin{bmatrix} \frac{\bar{q}SC\beta}{m}(C_{Xo}C_\alpha + C_{Zo}S_\alpha) \\ \frac{\bar{q}S}{mVC_\beta}(C_{Zo}C_\alpha - C_{Xo}S_\alpha) \\ -\frac{qSS\beta}{mV}(C_{Xo}C_\alpha + C_{Zo}S_\alpha) \end{bmatrix} + \begin{bmatrix} C_\theta S_\phi S_\beta - S_\theta C_\alpha C_\beta + C_\theta C_\phi S_\alpha C_\beta \\ \frac{1}{VC_\beta}(C_\alpha C_\theta C_\phi + S_\theta S_\alpha) \\ \frac{1}{V}(C_\theta S_\phi C_\beta + S_\beta C_\theta C_\alpha - C_\theta C_\phi S_\alpha S_\beta) \end{bmatrix} g \quad (57)$$

Here,  $S_\alpha$ ,  $C_\alpha$ ,  $S_\beta$ ,  $C_\beta$ ,  $S_\phi$ ,  $C_\phi$ ,  $S_\theta$ , and  $C_\theta$  denote  $\sin \alpha$ ,  $\cos \alpha$ ,  $\sin \beta$ , and so on.

The gravity term in Eq. (57) can be partitioned into  $\theta$  and  $\phi$  terms using polynomial expressions of  $\cos$  and  $\sin$  functions. In this report,

$$\begin{aligned} \cos(x) &\cong 1 + b_1x^2 + b_2x^4 \\ \sin(x) &\cong a_1x + a_2x^3 + a_3x^5 \end{aligned}$$

The gravity term can be written as:

$$\begin{bmatrix} g_{v\theta}g & g_{v\phi}g \\ \frac{g}{V C_\beta} g_{\alpha\theta} & \frac{g}{V C_\beta} g_{\alpha\phi} \\ \frac{g}{V} g_{\beta\theta} & \frac{g}{V} g_{\beta\phi} \end{bmatrix} \begin{bmatrix} \theta \\ \phi \end{bmatrix} + \begin{bmatrix} S_\alpha C_\beta \\ \frac{1}{V C_\beta} C_\alpha \\ -\frac{1}{V} S_\alpha S_\beta \end{bmatrix} g \quad (58)$$

where

$$g_{v\theta} = -(a_1 + a_2\theta^2 + a_3\theta^4)C_\alpha C_\beta + (b_1\theta + b_2\theta^3)S_\alpha C_\beta \quad (59)$$

$$g_{v\phi} = (a_1 + a_2(1 + b_1\theta^2)\phi^2 + a_1b_1\theta^2 + a_1b_2\theta^4)S_\beta + ((b_1 + b_1^2\theta^2)\phi + b_2\phi^3)S_\alpha C_\beta \quad (60)$$

$$g_{\alpha\theta} = (a_1 + a_2\theta^2 + a_3\theta^4)S_\alpha + (b_1\theta + b_2\theta^3)C_\alpha \quad (61)$$

$$g_{\alpha\phi} = (b_1\phi + b_2\phi^3 + b_1^2\theta^2\phi)C_\alpha \quad (62)$$

$$g_{\beta\theta} = (b_1\theta + b_2\theta^3)C_\alpha S_\beta - (b_1\theta + b_2\theta^3)S_\alpha S_\beta \quad (63)$$

$$g_{\beta\phi} = (a_1 + a_2(1 + b_1\theta^2)\phi^2 + a_3\phi^4 + a_1b_1\theta^2 + a_1b_2\theta^4)C_\beta - (b_1\phi + b_2\phi^3 + b_1^2\theta^2\phi)S_\alpha S_\beta \quad (64)$$

The moment equation is written as:

$$\begin{bmatrix} \dot{p} \\ \dot{q} \\ \dot{r} \end{bmatrix} = J^{-1}A_m[V \ \alpha \ \beta \ p \ q \ r]^T + J^{-1}B_m[T \ \delta_e \ \delta_{ra} \ \delta_{la} \ \delta_{rf} \ \delta_{lf} \ \delta_r]^T + J^{-1}h_m \quad (65)$$

where

$$A_m = \begin{bmatrix} 0 & 0 & \bar{q}SbC_{l_\beta} & \frac{\bar{q}Sb^2}{2V}C_{l_p} + J_{zx}q - J_{xy}r & J_{yz}q - J_{zz}r & \frac{\bar{q}Sb^2}{2V}C_{l_r} + J_{yy}q - J_{yz}r \\ 0 & 0 & 0 & J_{zz}r - J_{zx}p & \frac{\bar{q}Sc^2}{2V}C_{m_q} + J_{xy}r - J_{yz}p & J_{zx}r - J_{xx}p \\ 0 & 0 & \bar{q}SbC_{n_\beta} & \frac{\bar{q}Sb^2}{2V}C_{n_p} + J_{xy}p - J_{yy}q & J_{xx}p - J_{xy}q & \frac{\bar{q}Sb^2}{2V}C_{n_r} + J_{yz}p - J_{zx}q \end{bmatrix} \quad (66)$$

$$B_m = \bar{q}S \begin{bmatrix} b & 0 & 0 \\ 0 & \bar{c} & 0 \\ 0 & 0 & b \end{bmatrix} \begin{bmatrix} 0 & 0 & C_{l_{\delta_{ra}}} & C_{l_{\delta_{la}}} & C_{l_{\delta_{rf}}} & C_{l_{\delta_{lf}}} & C_{l_{\delta_r}} \\ 0 & C_{m_{\delta_e}} & C_{m_{\delta_{ra}}} & C_{m_{\delta_{la}}} & C_{m_{\delta_{rf}}} & C_{m_{\delta_{lf}}} & C_{m_{\delta_r}} \\ 0 & 0 & C_{n_{\delta_{ra}}} & C_{n_{\delta_{la}}} & C_{n_{\delta_{rf}}} & C_{n_{\delta_{lf}}} & C_{n_{\delta_r}} \end{bmatrix} \quad (67)$$

and

$$h_m = \begin{bmatrix} 0 \\ \bar{q}S\bar{c}C_{m_o} \\ 0 \end{bmatrix} \quad (68)$$

Using Eqs (51) and (65), the full nonlinear equations of motion are written as:

$$\dot{X}_{st} = A(V, \alpha, \beta, p, q, r, \theta, \phi)X_{st} + B(V, \alpha, \beta)U + h(V, \alpha, \beta) \quad (69)$$

Here,

$$A(X_{st}) = \begin{bmatrix} I_{3 \times 3} & 0_{3 \times 3} & 0_{3 \times 2} \\ 0_{3 \times 3} & J^{-1} & 0_{3 \times 2} \\ 0_{2 \times 3} & 0_{2 \times 3} & I_{2 \times 2} \end{bmatrix} \begin{bmatrix} A_{force} & A_g \\ A_m & 0_{3 \times 2} \\ A_{tp} & 0_{2 \times 2} \end{bmatrix} \quad (70)$$

where

$$A_{tp} = \begin{bmatrix} 0 & 0 & 0 & 0 & C_\phi & -S_\phi \\ 0 & 0 & 0 & 1 & S_\phi \tan \theta & C_\phi \tan \theta \end{bmatrix} \quad (71)$$

and

$$A_g = \begin{bmatrix} g_{v\theta}g & g_{v\phi}g \\ \frac{g}{\sqrt{C_\beta}}g_{\alpha\theta} & \frac{g}{\sqrt{C_\beta}}g_{\alpha\phi} \\ \frac{g}{\sqrt{V}}g_{\beta\theta} & \frac{g}{\sqrt{V}}g_{\beta\phi} \end{bmatrix} \quad (72)$$

$$B = \begin{bmatrix} I_{3 \times 3} & 0_{3 \times 3} & 0_{3 \times 2} \\ 0_{3 \times 3} & J^{-1} & 0_{3 \times 2} \\ 0_{2 \times 3} & 0_{2 \times 3} & I_{2 \times 2} \end{bmatrix} \begin{bmatrix} B_{force} \\ B_m \\ 0_{2 \times 7} \end{bmatrix} \quad (73)$$

and

$$h = \begin{bmatrix} I_{3 \times 3} & 0_{3 \times 3} & 0_{3 \times 2} \\ 0_{3 \times 3} & J^{-1} & 0_{3 \times 2} \\ 0_{2 \times 3} & 0_{2 \times 3} & I_{2 \times 2} \end{bmatrix} \begin{bmatrix} h_{force} \\ h_m \\ 0_{2 \times 1} \end{bmatrix} \quad (74)$$

## APPENDIX B

### Matrix Form of Longitudinal Motion

Consider longitudinal motion only. To extract the longitudinal motion from full equation of motion in Eq. (69), the state values related to lateral-directional motion are set to zero and the components ( $J_{yx}$ ,  $J_{yz}$ ) of inertia moment matrix  $J$  are set as zero because of symmetric configuration about the x-z plane. The longitudinal motion is rewritten as

$$\begin{bmatrix} \dot{V} \\ \dot{\alpha} \\ \dot{q} \\ \dot{\theta} \end{bmatrix} = A_{lon}(V, \alpha) \begin{bmatrix} V \\ \alpha \\ q \\ \theta - \theta_0 \end{bmatrix} + B_{lon}(V, \alpha) \begin{bmatrix} T \\ \delta_e \\ \delta_{a_{all}} \\ \delta_{f_{all}} \end{bmatrix} + h_{lon}(V, \alpha) \quad (75)$$

where

$$A_{lon} = \begin{bmatrix} 0 & 0 & \frac{\bar{q}S\bar{c}}{2mV}(C_{x_q}C_\alpha + C_{z_q}S_\alpha) & g(-C_\alpha \cos \theta_0 - S_\alpha \sin \theta_0) \\ 0 & 0 & 1 + \frac{\bar{q}S\bar{c}}{2mV^2}(C_{z_q}C_\alpha - C_{x_q}S_\alpha) & g(S_\alpha \cos \theta_0 - C_\alpha \sin \theta_0)/V \\ 0 & 0 & \frac{\bar{q}S\bar{c}^2}{2VJ_{yy}}C_{m_q} & 0 \\ 0 & 0 & 1 & 0 \end{bmatrix} \quad (76)$$

Recall that the longitudinal control surfaces of this airplane are thrust, an elevator, ailerons and flaps. The matrix  $B_1$  and  $B_2$  are for the conventional control surface ( $T, \delta_e$ ) and for the ailerons and flaps, respectively.

$$B_{lon} = [B_1 \ B_2] \quad (77)$$

where

$$B_1 = \begin{bmatrix} \frac{C_\alpha}{m} & \frac{\bar{q}S}{m}(C_{x_{\delta_e}}C_\alpha + C_{z_{\delta_e}}S_\alpha) \\ -\frac{S_\alpha}{mV} & \frac{\bar{q}S}{mV}(C_{z_{\delta_e}}C_\alpha - C_{x_{\delta_e}}S_\alpha) \\ 0 & \frac{\bar{q}S\bar{c}}{J_{yy}}C_{m_{\delta_e}} \\ 0 & 0 \end{bmatrix}$$

$$B_2 = \begin{bmatrix} \frac{qS}{m}(C_{x_{\delta_a}}C_\alpha + C_{z_{\delta_a}}S_\alpha) & \frac{qS}{m}(C_{x_{\delta_f}}C_\alpha + C_{z_{\delta_f}}S_\alpha) \\ \frac{\bar{q}S}{mV}(C_{z_{\delta_a}}C_\alpha - C_{x_{\delta_a}}S_\alpha) & \frac{\bar{q}S}{mV}(C_{z_{\delta_f}}C_\alpha - C_{x_{\delta_f}}S_\alpha) \\ \frac{\bar{q}S\bar{c}}{J_{yy}}C_{m_{\delta_a}} & \frac{\bar{q}S\bar{c}}{J_{yy}}C_{m_{\delta_f}} \\ 0 & 0 \end{bmatrix}$$

The nonlinear components of  $h$  are rewritten as

$$h_{lon} = \begin{bmatrix} \frac{\bar{q}S}{m}(C_{x_o}C_\alpha + C_{z_o}S_\alpha) + g(-C_\alpha \sin \theta_0 + S_\alpha \cos \theta_0) \\ \frac{\bar{q}S}{mV}(C_{z_o}C_\alpha - C_{x_o}S_\alpha) + g(S_\alpha \sin \theta_0 + C_\alpha \cos \theta_0)/V \\ \frac{\bar{q}S\bar{c}}{J_{yy}}C_{m_o}(\alpha) \\ 0 \end{bmatrix}$$

Note that the aerodynamic stability derivatives are functions of angle of attack  $\alpha$ .

### Matrix Form of Lateral-Directional Motion

Under assumption that  $q$  is zero and  $V$ ,  $\alpha$ , and  $\theta$  are at a trim condition, lateral-directional motion can be extracted from Eq.(69). The lateral-directional motion can be rewritten as:

$$\dot{X}_{lat} = A_{lat}(V, \alpha, \beta, \theta, \phi)X_{lat} + B_{lat}(V, \alpha, \beta)U_{lat} \quad (78)$$

Here,

$$A_{lat} = \begin{bmatrix} A_\beta \\ A_{pr} \\ A_\phi \end{bmatrix}, \quad B_{lat} = \begin{bmatrix} B_\beta \\ B_{pr} \\ B_\phi \end{bmatrix} \quad (79)$$

where

$$\begin{aligned} A_\beta &= \left[ \frac{\bar{q}SC_\beta C_{Y_\beta}}{mV} (S_\alpha + \frac{\bar{q}SbC_\beta}{2mV^2}C_{Y_p}) \quad (-C_\alpha + \frac{\bar{q}SbC_\beta}{2mV^2}C_{Y_r}) \quad \frac{g}{V}g_{\beta\phi} \right] \\ A_{pr} &= J_{sub}^{-1} \begin{bmatrix} \bar{q}SbC_{l_\beta} & \frac{\bar{q}Sb^2}{2V}C_{l_p} & \frac{\bar{q}Sb^2}{2V}C_{l_r} & 0 \\ \bar{q}SbC_{n_\beta} & \frac{\bar{q}Sb^2}{2V}C_{n_p} & \frac{\bar{q}Sb^2}{2V}C_{n_r} & 0 \end{bmatrix} \\ A_\phi &= [0 \quad 1 \quad C_\phi \tan \theta \quad 0] \\ B_\beta &= \left[ \frac{\bar{q}S}{mV}(C_\beta Y_{\delta_{aas}} - C_\alpha S_\beta C_{X_{\delta_{aas}}} - S_\beta S_\alpha C_{Z_{\delta_{aas}}}) \quad \frac{\bar{q}S}{mV}(C_\beta Y_{\delta_{fas}} - C_\alpha S_\beta C_{X_{\delta_{fas}}} - S_\beta S_\alpha C_{Z_{\delta_{fas}}}) \quad C_\beta C_{Y_{\delta_r}} \right] \\ B_{pr} &= \bar{q}SbJ_{sub}^{-1} \begin{bmatrix} C_{l_{\delta_{aas}}} & C_{l_{\delta_{fas}}} & C_{l_{\delta_r}} \\ C_{n_{\delta_{aas}}} & C_{n_{\delta_{fas}}} & C_{n_{\delta_r}} \end{bmatrix} \\ B_\phi &= [0 \quad 0 \quad 0] \end{aligned} \quad (80)$$

and

$$J_{sub} = \begin{bmatrix} J_{xx} & -J_{xz} \\ -J_{xz} & J_{zz} \end{bmatrix} \quad (81)$$

## APPENDIX C

### Characteristic Polynomial for Longitudinal Motion

The characteristic polynomial of the matrix  $A_f$  described in Eq. (46) is written as

$$s^4 + \tilde{a}s^3 + \tilde{b}s^2 + \tilde{c}s + \tilde{d}.$$

The coefficients  $\tilde{a}$ ,  $\tilde{b}$ ,  $\tilde{c}$  and  $\tilde{d}$  are follows:

$$\tilde{a} = g_a^T x$$

where  $g_a^T = [-(a_{11}^p + a_{22}^p + a_{33}^p) \quad -n_1 \quad -n_2 \quad 0]$  and  $x^T = [1 \quad \phi_1 \quad \phi_2 \quad \phi_3]$ . Recall that  $n_1$  and  $n_2$  are the elements of the nullspace  $\mathcal{N}$ . The coefficient  $\tilde{b}$  is

$$\tilde{b} = g_b^T x = [\tilde{b}_0 \quad \tilde{b}_1 \quad \tilde{b}_2 \quad \tilde{b}_3]x$$

where

$$\begin{aligned} \tilde{b}_0 &= (a_{22}^p + a_{11}^p)a_{33}^p - a_{32}^p a_{23}^p + a_{11}^p a_{22}^p - a_{21}^p a_{12}^p - a_{31}^p a_{13}^p \\ \tilde{b}_1 &= (a_{22}^p + a_{33}^p)n_1 - a_{21}^p n_2 \\ \tilde{b}_2 &= (a_{33}^p + a_{11}^p)n_2 - a_{12}^p n_1 \\ \tilde{b}_3 &= -a_{23}^p n_2 - a_{13}^p n_1. \end{aligned}$$

The coefficient  $\tilde{c}$  is

$$\tilde{c} = g_c^T x = [\tilde{c}_0 \quad \tilde{c}_1 \quad \tilde{c}_2 \quad \tilde{c}_3]x$$

where

$$\begin{aligned} \tilde{c}_0 &= (a_{21}^p a_{12}^p - a_{11}^p a_{22}^p)a_{33}^p + (a_{31}^p a_{22}^p - a_{21}^p a_{32}^p)a_{13}^p \\ &\quad + (a_{11}^p a_{23}^p - a_{24}^p)a_{32}^p - (a_{14}^p + a_{23}^p a_{12}^p)a_{31}^p \\ \tilde{c}_1 &= (a_{32}^p a_{23}^p - a_{33}^p a_{22}^p)n_1 + (a_{21}^p a_{33}^p - a_{31}^p a_{23}^p)n_2 \\ \tilde{c}_2 &= (a_{12}^p a_{33}^p - a_{32}^p a_{13}^p)n_1 - (a_{31}^p a_{13}^p - a_{11}^p a_{33}^p)n_2 \\ \tilde{c}_3 &= (a_{13}^p a_{22}^p - a_{23}^p a_{12}^p - a_{14}^p)n_1 \\ &\quad + (a_{11}^p a_{23}^p - a_{21}^p a_{13}^p - a_{24}^p)n_2. \end{aligned}$$

The coefficient  $\tilde{d}$  is

$$\tilde{d} = g_d^T x = [\tilde{d}_0 \quad \tilde{d}_1 \quad \tilde{d}_2 \quad \tilde{d}_3]x$$

where

$$\begin{aligned} \tilde{d}_0 &= (a_{11}^p a_{32}^p - a_{31}^p a_{12}^p)a_{24}^p + (a_{31}^p a_{22}^p - a_{21}^p a_{32}^p)a_{14}^p \\ \tilde{d}_1 &= a_{24}^p a_{32}^p n_1 - a_{31}^p a_{24}^p n_2 \\ \tilde{d}_2 &= a_{31}^p a_{14}^p n_2 - a_{32}^p a_{14}^p n_1 \\ \tilde{d}_3 &= (a_{22}^p a_{14}^p - a_{12}^p a_{24}^p)n_1 + (a_{11}^p a_{24}^p - a_{21}^p a_{14}^p)n_2. \end{aligned}$$

## ACKNOWLEDGMENTS

The author thanks the technical monitor Dr. Christine Belcastro at NASA Langley Research Center and also acknowledges the contributions of Dr. David Cox (NASA Langley Research Center), and Pawel Chwalowski (Analytic Mechanics Associates) for developing the nonlinear dynamics of the aircraft.

## REFERENCES

- [1] AeroLogic Inc. *CMARC V4.0: Three-Dimensional Low Order Panel Code*, 1995.
- [2] Apkarian, P. and Adams, R. Advanced Gain-Scheduling Techniques for Uncertain Systems. *IEEE Transactions on Control Systems Technology*, 6(1):21–32, 1998.
- [3] Balas, G., Fialho, I., Packard, A., Renfrow, J., and Mullaney, C. On the Design of LPV Controllers for the F-14 Aircraft Lateral-Directional Axis During Powered Approach. In *Proceedings of the American Control Conference*, pages 123–127, Albuquerque, NM, 1997.
- [4] Balas, G., Ryan, J., Shin, J-Y., and Garrard, W. A New Technique for Design of Controllers for Turbofan Engines. In *AIAA 34th Joint Propulsion Conference*, pages 1–6, Cleveland, OH, 1998. AIAA-98-3751.
- [5] Balas, G., Packard, A., Renfrow, J., Mullaney, C., and M’Closky, R. Control of the F-14 Aircraft Lateral-Directional Axis During Powered Approach. *Journal of Guidance, Control, and Dynamics*, 21(6):899–908, Nov. 1998.
- [6] Becker, G. *Quadratic Stability and Performance of Linear Parameter Dependent Systems*. PhD thesis, Department of Engineering, University of California, Berkeley, 1993.
- [7] Etkin, B. and Reid, L. *Dynamics of Flight Stability and Control*. John Wiley and Sons Inc., 1996.
- [8] Gloudeman, J.R. and Kinney D. *Vorview Verison 2.0*. Lawrence Pierce and NASA Ames, Aug. 2001.
- [9] Khalil, H. *Nonlinear Systems*. Prentice Hall Inc, second edition, 1996.
- [10] Kwatny, H. and Chang, B-C. Constructing Linear Families from Parameter-Dependent Nonlinear Dynamics. *IEEE Transactions on Automatic Control*, 43(8):1143–1147, 1998.
- [11] Löfberg, J. <http://control.ee.ethz.ch/~joloef/yalmip.php>.
- [12] Lee, S-H. and Lim, J-T. Fast Gain Scheduling on Tracking Problem Using Derivative Information. *Automatica*, 33(12):2265–2268, 1997.

- [13] Leith, D.J. and Leithead, W.E. Comments on the Prevalence of Linear Parameter Varying Systems. Technical report, Department Electronic and Electrical Engineering, University of Strathclyde, Glasgow, Scotland, 1999.
- [14] Lim, S. and How, J. Control of LPV Systems Using a Quasi-Piecewise Affine Parameter-Dependent Lyapunov Function. In *Proceedings of the American Control Conference*, pages 1200–1204, Philadelphia, PA, 1998.
- [15] Marcos, A. and Balas, G. Linear Parameter Varying Modeling of the Boeing 747-100/200 Longitudinal Motion. In *AIAA Guidance, Navigation and Control Conference*, AIAA-01-4347, Montreal, Canada, Aug. 2001. American Institute of Aeronautics and Astronautics.
- [16] Monzon, B.R. Development of a Nonlinear Simulation for a Research Model Airplane. Master’s thesis, MSE Thesis, George Washington University JIAFS., NASA Langley Research Center, September 2001.
- [17] Morelli, E.A. and DeLoach, R. Wind Tunnel Database Development using Modern Experiment Design and Multivariate Orthogonal Functions. In *41<sup>st</sup> AIAA Aerospace Sciences Meeting and Exhibit*, number AIAA 2003-0653, Reno, NV, Jan. 6-9 2003. American Institute of Aeronautics and Astronautics.
- [18] Ogunnaike, B.A. and Ray, W.H. *Process Dynamics Modeling and Control*. Oxford University Press, New York, Oxford, 1994. Ch. 14. pp. 486–492.
- [19] P. Chwalowski. Vehicle Configuration Studies and Small Aircraft Formation Flying Study. Technical Report 04-33, Analytical Mechanics Associates, Inc., Nov. 2004.
- [20] Papageorgiou, G. *Robust Control System Design  $\mathcal{H}_\infty$  Loop Shaping and Aerospace Application*. PhD thesis, Department of Engineering, University of Cambridge, 1998.
- [21] Rodrigues, L. *Dynamic Output Feedback Controller Synthesis for Piecewise-Affine Systems*. PhD thesis, Department of Aeronautics and Astronautics, Stanford University, 2002.
- [22] Rugh, J. Analytical Framework for Gain Scheduling. *IEEE Control Systems Magazine*, 11:1215–1219, 1991.
- [23] Shamma, J. and Athans, M. Guaranteed Properties of Gain Scheduled Control for Linear Parameter-Varying Plants. *Automatica*, 35(8):559–564, 1991.
- [24] Shamma, J. and Cloutier, J. Gain-Scheduled Missile Autopilot Design Using Linear Parameter Varying Transformations. *Journal of Guidance, Control, and Dynamics*, 16(2):256–261, 1993.

- [25] Shin, J-Y. *Worst-case Analysis and Linear Parameter Varying Control of Aerospace System*. PhD thesis, Department of Aerospace Engineering and Mechanics, University of Minnesota, 2000.
- [26] Shin, J-Y., Balas, G.J., and Kaya, M.A. Blending Methodology of Linear Parameter Varying Control Synthesis of F-16 Aircraft System. *Journal of Guidance, Control, and Dynamics*, 25(6):1040–1048, 2002.
- [27] Smith, S., Reuther, J., Kinney D., and Saunders D. Low Speed Aerodynamics and Landing Characteristics of Sharp-Class Crew Transfer Vehicle Concepts. In *AIAA Thermophysics Conference*. AIAA, AIAA, June 2001. AIAA2001-2888.
- [28] Stilwell, D. and Rugh, W. Interpolation of Observer State Feedback Controller for Gain Scheduling. In *Proceedings of the American Control Conference*, pages 1215–1219, Philadelphia, PA, 1998.
- [29] Tan, W. Applications of Linear Parameter-Varying Control Theory. Master’s thesis, Department of Mechanical Engineering, University of California at Berkeley, 1997.
- [30] Tan, W., Packard, A., and Balas, G. Quasi-LPV Modeling and LPV Control of a Generic Missile. In *Proceedings of the American Control Conference*, pages 3692–3696, Chicago, IL, 2000.
- [31] Wolodkin, G., Balas, G., and Garrard, W. Application to Parameter Dependent Robust Control Synthesis to Turbofan Engines. In *AIAA, Aerospace Sciences Meeting and Exhibit*, AIAA-98-0973, Reno, NV, 1998.
- [32] Wu, F. *Control of Linear Parameter Varying Systems*. PhD thesis, Department of Mechanical Engineering, University of California, Berkeley, 1995.
- [33] Wu, F., Packard, A., and Balas, G. LPV Control Design for Pitch-Axis Missile Autopilots. In *Proceedings of the 34th Conference on Decision and Control*, pages 188–193, New Orleans, LA, 1995.
- [34] Zhou, K., Doyle, J., and Glover, K. *Robust and Optimal Control*. Prentice Hall, New Jersey, 1996.

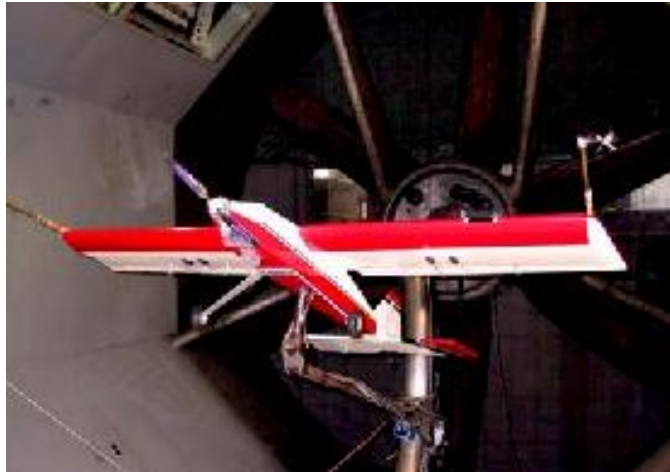


Figure 1: *The FASER*

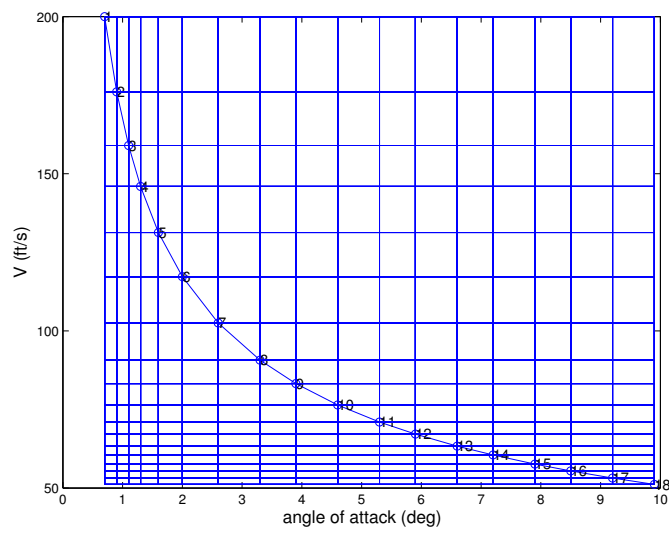


Figure 2: *The numbered equilibrium points and grid points*

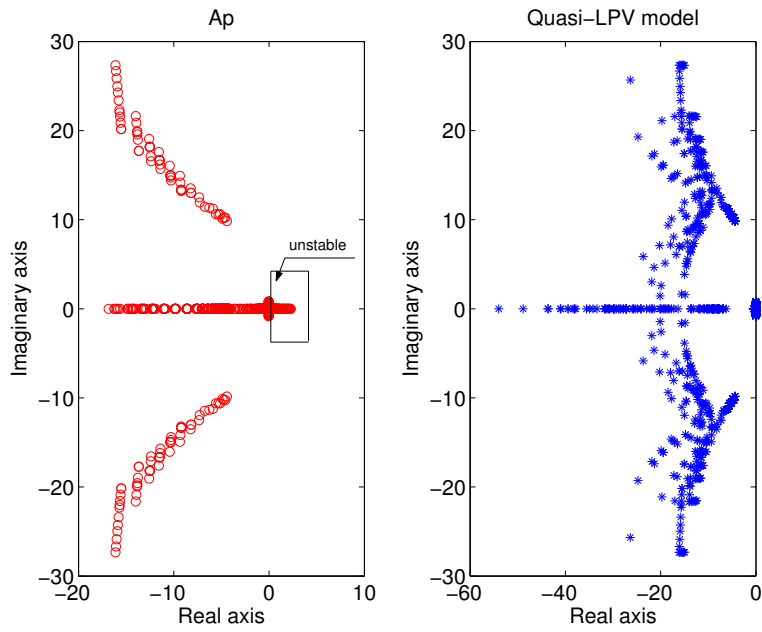


Figure 3: *Eigenvalues of particular solution  $A_p$  and the matrix  $A$  of the quasi-LPV model*

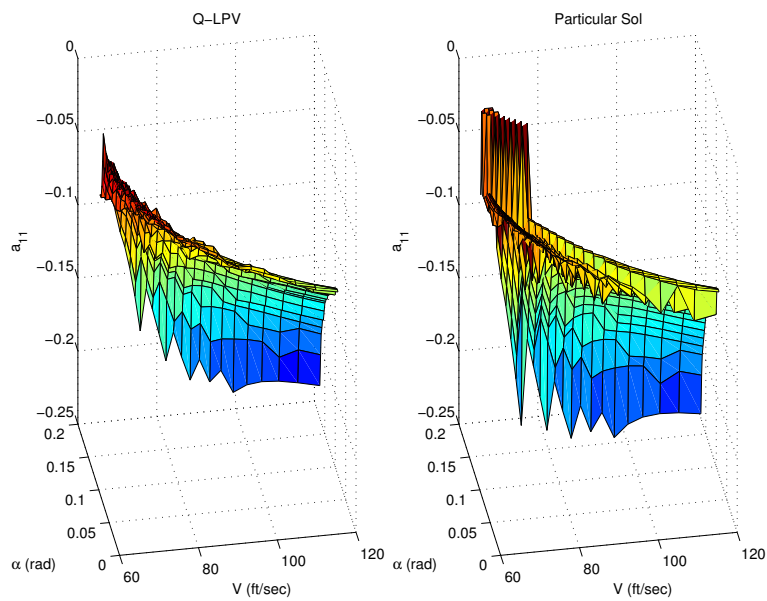


Figure 4: *Variation of  $a_{11}$  element of the matrix  $A_f$*

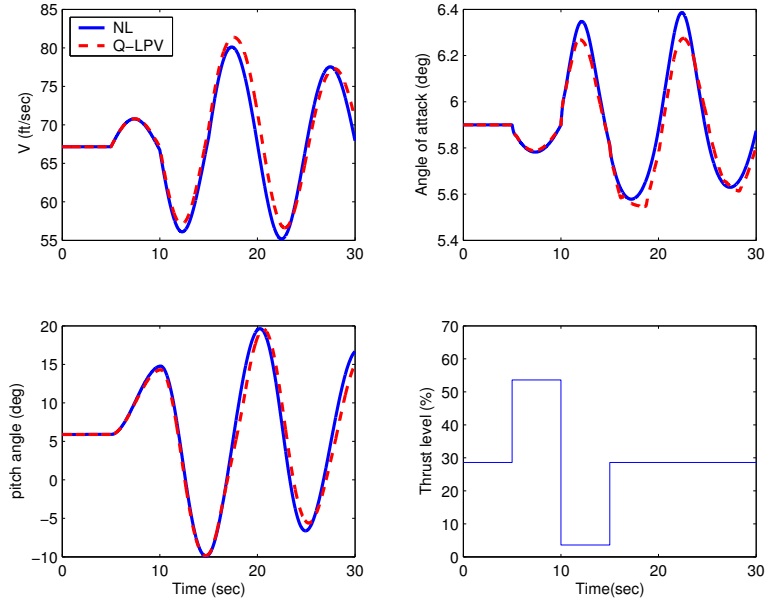


Figure 5: *Time responses due to the thrust level change.*

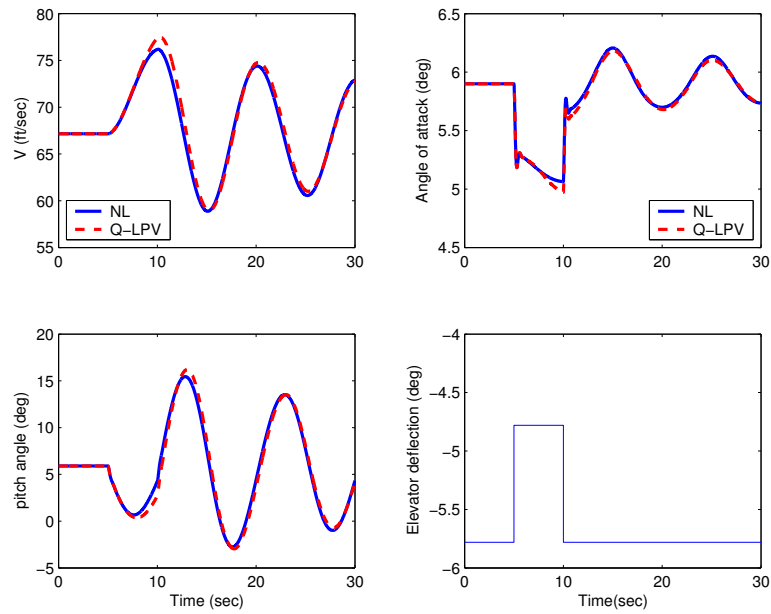


Figure 6: *Time responses due to the elevator deflection change.*

